EPSIN1 and MTV1 define functionally overlapping but molecularly distinct *trans*-Golgi network subdomains in *Arabidopsis*

Laura Heinze[a], Nina Freimuth[a], Ann-Kathrin Rößling[a], Reni Hahnke[a], Sarah Riebschläger[a], Anja Fröhlich[b], Arun Sampathkumar[b], Heather E. McFarlane[c,d], and Michael Sauer[a,1]

[a]Department of Plant Physiology, University of Potsdam, 14476 Potsdam, Germany; [b]Max Planck Institute of Molecular Plant Physiology, 14476 Potsdam, Germany; [c]School of Biosciences, University of Melbourne, Melbourne, VIC 3010, Australia; and [d]Department of Cell and Systems Biology, University of Toronto, Toronto, ON M5S 3G5, Canada

Edited by Natasha V. Raikhel, Center for Plant Cell Biology, Riverside, CA, and approved August 27, 2020 (received for review March 13, 2020)

The plant *trans*-Golgi network (TGN) is a central trafficking hub where secretory, vacuolar, recycling, and endocytic pathways merge. Among currently known molecular players involved in TGN transport, three different adaptor protein (AP) complexes promote vesicle generation at the TGN with different cargo specificity and destination. Yet, it remains unresolved how sorting into diverging vesicular routes is spatially organized. Here, we study the family of *Arabidopsis thaliana* Epsin-like proteins, which are accessory proteins to APs facilitating vesicle biogenesis. By comprehensive molecular, cellular, and genetic analysis of the EPSIN gene family, we identify EPSIN1 and MODIFIED TRANSPORT TO THE VACUOLE1 (MTV1) as its only TGN-associated members. Despite their large phylogenetic distance, they perform overlapping functions in vacuolar and secretory transport. By probing their relationship with AP complexes, we find that they define two molecularly independent pathways: While EPSIN1 associates with AP-1, MTV1 interacts with AP-4, whose function is required for MTV1 recruitment. Although both EPSIN1/AP-1 and MTV1/AP-4 pairs reside at the TGN, high-resolution microscopy reveals them as spatially separate entities. Our results strongly support the hypothesis of molecularly, functionally, and spatially distinct subdomains of the plant TGN and suggest that functional redundancy can be achieved through parallelization of molecularly distinct but functionally overlapping pathways.

intracellular protein transport | ENTH domain | Epsins | adaptor complexes | *trans*-Golgi network

The *trans*-Golgi network (TGN) is a major sorting hub of the plant endosomal system. It is a blebbing, tubular-reticular membrane structure usually found in close vicinity to the *trans* side of Golgi stacks, from which it originates (1). At least four important pathways merge at this morphologically and functionally independent entity. This includes the anterograde routes of secretory, recycling, and vacuolar transport, as well as the retrograde endocytic pathway (reviewed in ref. 2). All instances of cargo exit and entry involve mobile vesicles. Given the wide range of cargo types and destinations, it is currently not clear how sorting of cargo and distribution into different vesicles are organized at the molecular level. A current hypothesis in the field is the presence of distinct TGN subdomains with differing molecular makeup and cargo affinity that define specific transport routes. There is some evidence hinting at the presence of such subdomains or molecularly distinct TGN populations (3–7), but many details remain unclear.

Controlled exit from the TGN requires molecular machinery to recognize, sort, and pack cargo proteins into vesicles. Adaptor protein (AP) complexes and their associated accessory proteins of the Epsin type are important components for clathrin-coated vesicle (CCV) generation. AP complexes are heterotetrameric complexes that are recruited to sites of incipient CCV formation and serve as molecular bridges between cargo receptors and clathrin coat components. They sort and concentrate cargo into clathrin-coated pits and also contribute to the actual coat formation. In *Arabidopsis*, four functional AP complexes, AP-1 through AP-4, have been reported. A fifth, AP-5, complex might be missing in land plants because the AP-5 σ-subunit appears to have been lost (8). While many details still await elucidation, the general roles of the APs are endocytosis at the plasma membrane (PM) (AP-2) and anterograde transport of cargo from the TGN to the vacuoles/tonoplast as well as the apoplast/PM (AP-1, AP-3, AP-4) (reviewed in ref. 9). Although functional differences are known, the molecular details are only slowly emerging.

In contrast to APs, little is known about plant Epsin-type accessory proteins. Most of our knowledge stems from studies of their conserved counterparts in animals and yeast. Generally, Epsins interact with the appendage/ear domains of large adaptin subunits present in all APs (10). The large, unstructured C-terminal part of Epsins contains motifs for this interaction as well as for interaction with clathrin. The N terminus contains an Epsin N-terminal homology (ENTH) domain that recognizes specific phosphoinositides in the donor membrane, triggering a conformational change that leads to partial insertion of an α-0-helix into the cytoplasmic leaflet (11). This facilitates membrane bulging and might also exert destabilizing functions to enable scission of the vesicle (12, 13). Furthermore, Epsins can interact with ubiquitin, certain types of cargo molecules, and actin, making them versatile adaptor/accessory proteins in vesicular transport (reviewed in ref. 14).

Significance

This is a comprehensive study of Epsin-like accessory proteins in *Arabidopsis*, for which so far only limited data are available. We identify two members as major accessory proteins at the TGN, controlling vacuolar and a subset of secretory transport. By interaction studies with AP complexes, genetic interactions, and enhanced-resolution microscopy, our work reveals the existence of two independent, parallel transport pathways, which originate from spatially separate regions at the TGN. Our study thus provides strong molecular, cellular, and genetic evidence for spatially, functionally, and molecularly separate subdomains of the plant TGN.

Author contributions: L.H., A.S., H.E.M., and M.S. designed research; L.H., N.F., A.-K.R., R.H., S.R., A.F., A.S., H.E.M., and M.S. performed research; L.H., N.F., A.-K.R., R.H., S.R., H.E.M., and M.S. analyzed data; and L.H., H.E.M., and M.S. wrote the paper.

The authors declare no competing interest.

This article is a PNAS Direct Submission.

[1]To whom correspondence may be addressed. Email: michael.sauer@uni-potsdam.de.

This article contains supporting information online at https://www.pnas.org/lookup/suppl/doi:10.1073/pnas.2004822117/-/DCSupplemental.

First published September 28, 2020.

Arabidopsis contains several proteins with an ENTH domain (15) (Fig. 1*A*), whose functional roles and exact localizations are only partially described. EPSIN1/EPSIN1R was found in endosomal structures of unclear identity and may play a role in protein delivery to vacuoles (16) and a subset of PM proteins (17). The phylogenetically distant MODIFIED TRANSPORT TO THE VACUOLE1 (MTV1) was found at the TGN, with a clear role in vacuolar transport (18). For the remaining ENTH-type accessory proteins, there are no definite data on their localization or function. Here, we present a comprehensive analysis of all *Arabidopsis* Epsin-like proteins. We find that they split into two groups based on their localization: PM and TGN. The two TGN members both perform widely overlapping functions in vacuolar and secretory transport. Surprisingly, they nevertheless associate with different AP complexes and reside on spatially separate parts of the TGN. Our work provides strong microscopic, biochemical, and genetic evidence for the existence of the TGN subdomains and sheds light on the functional specialization of the so far underresearched accessory proteins.

Results

Based on Subcellular Localization, ENTH Proteins Can Be Sorted into Two Groups. A phylogenetic analysis of all ENTH-like proteins across diverse plant taxa revealed that *Arabidopsis* contains four proteins with ENTH domains and long, unstructured C-terminal tails (Fig. 1*A*) (15). Three of them are closely related and include EPSIN1/EPSINR1 (16), EPSIN2 (19), and the so far uncharacterized EPSIN3. The remaining ENTH protein, MTV1, is a phylogenetic outlier, but remarkably conserved throughout plant taxa (18). Three other ENTH domain proteins possess truncated C termini of only around 100 amino acids (Fig. 1*A*, short ENTH proteins). These are not included in this study, because they lack any detectable clathrin or AP complex interaction sites and likely have other functions (15).

In order to functionally classify the four large ENTH proteins EPSIN1 to 3 and MTV1, we first addressed their subcellular localization by generating transgenic lines that stably expressed functional, fluorescently (enhanced green fluorescent protein [EGFP] or mRuby3) tagged proteins under control of their endogenous promoters. Using root epidermal cells as an established model system, we observed two clearly distinct localization patterns: EPSIN1-GFP and MTV1-GFP were found in speckles reminiscent of endosomal structures (Fig. 1*B*), while EPSIN2 and EPSIN3 were found predominantly at the PM and also at the cell plate in dividing cells (Fig. 1*B*, arrowheads). Thus, subcellular localization alone helped to identify at least two groups of likely distinct function.

EPSIN1 and MTV1 Show Strong Genetic Interaction. For functional analyses, we isolated T-DNA insertion mutants of all four genes and confirmed their nullizygosity by qPCR (*SI Appendix*, Fig. S1). However, we did not observe drastic phenotypes in any of the single mutants (*SI Appendix*, Fig. S2), potentially indicating functional redundancy. For redundancy to occur, gene expression must spatiotemporally overlap. We therefore checked expression patterns in planta by generating C-terminally β-glucuronidase-tagged versions of all proteins under their endogenous promoters. All four genes are expressed in almost all plant tissues and developmental stages tested (*SI Appendix*, Fig. S3), with most variation found in floral organs. We conclude that, at least during vegetative development, there is substantial spatiotemporal overlap of expression, potentially allowing functional redundancy.

To address redundancy, we generated higher-order mutants and measured rosette area as a proxy for overall plant status. From all mutant combinations, only the *epsin1 mtv1* (*eps1 mtv1*) double mutant exhibited a drastic dwarf phenotype (Fig. 1 *C* and *D* and *SI Appendix*, Fig. S2), which was also reflected by reduced root length (Fig. 1*E*). From these results, we conclude that, despite their large phylogenetic distance, EPSIN1 and MTV1 form a functionally redundant pair of endosomal ENTH proteins. Since no other mutant combinations exhibited obvious phenotypes, we decided to focus our attention on these two members.

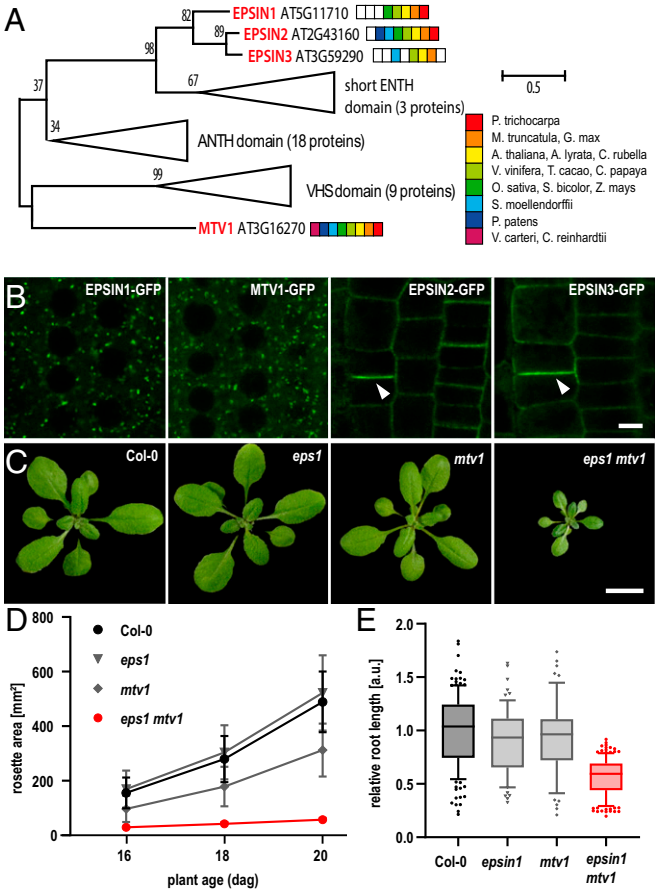

Fig. 1. EPSIN1 and MTV1 are the major endosomal ENTH proteins of *Arabidopsis*. (*A*) Phylogenetic analysis of ENTH domain-like proteins shows MTV1 is a highly conserved outlier. The Coulson plot shows the occurrence of at least one ortholog in the indicated taxa. (*B*) EPSIN1 and MTV1 show a punctate endosomal pattern; in contrast, EPSIN2 and EPSIN3 are at the PM and cell plates (arrowheads). Epidermal root cells of 5 d after germination (dag) plants expressing *pEPSIN1:EPSIN1-GFP*, *pMTV1:MTV1-GFP*, *pEPSIN2:EPSIN2-GFP*, and *pEPSIN3:EPSIN3-GFP*. (*C*–*E*) The double mutant *eps1 mtv1* has severely reduced growth. (*C*) Phenotypes of 24 dag rosettes of Col-0, *eps1*, *mtv1*, and the *eps1 mtv1* double mutant. (*D*) Rosette area over three time points, three experiments, with six to eight plants per genotype; plotted is the mean of means, and bars indicate range. (*E*) Root length of $58 < n < 146$ 7 dag plants per genotype from three experiments normalized to the respective Col-0 and then pooled; whiskers, 10 to 90%, with all outliers as points. a.u., arbitrary units. [Scale bars, substitutions per site (*A*), 10 μm (*B*), and 2 cm (*C*).]

EPSIN1 and MTV1 Are TGN-Associated Proteins. MTV1 is a TGN-localized protein (18), while the subcellular localization of EPSIN1 has not clearly been demonstrated in *Arabidopsis* tissue (16). To address its localization, we introgressed established fluorescent subcellular marker lines into the lines expressing functional *pEPSIN1:EPSIN1-GFP* or *pMTV1:MTV1-GFP*. We performed colocalization analyses using enhanced-resolution (Airyscan) confocal microscopy in conjunction with object-based quantification to measure the center–center distance of neighboring endosomal punctae [DiAna plugin for ImageJ (20)]. This method is advantageous over intensity correlation-based methods because it is relatively insensitive to background noise, does not require arbitrarily set intensity thresholds, and

PLANT BIOLOGY

does not discard punctae. Large populations of object pairs can be measured semiautomatically and we use the median distance from each object pair population as a proxy for the degree of colocalization. By defining and comparing the centers of larger objects, distance values can be smaller than the theoretical resolution limit (~150 nm in our setup).

Using the established TGN marker VHAa1-RFP (red fluorescent protein) (21), we observed relatively small median distances of 182 nm for EPSIN1 and 104 nm for MTV1 (Fig. 2 *A–C*). Moreover, the distributions were clearly skewed toward smaller values, indicating close proximity for the majority of objects. We also tested the clathrin light-chain marker CLC-mKO, which predominantly marks the TGN, albeit with minor portions of *trans*-Golgi cisternae and multivesiculate bodies (22). Again, we observed small distances close to or below the resolution limit (median 98 nm for EPSIN1 and 186 nm for MTV1) (Fig. 2 *D–F*). Other endosomal structures with similar, punctate localization patterns include the prevacuolar compartment (PVC) and the Golgi. We tested colocalization with these compartments using wave2R/mCherry-RabF2b for the PVC and wave22R/mCherry-SYP32 for the Golgi (23). Neither of them colocalized with EPSIN1-GFP or MTV1-GFP (Fig. 2 *G–L*). For the PVC, the distances between neighboring object centers distributed uniformly around medians of 341 and 343 nm for EPSIN1 and MTV1, respectively (Fig. 2 *G–I*). For the Golgi marker wave22R/mCherry-SYP32, we found 436 nm for EPSIN1 and 351 nm for EPSIN (Fig. 2 *J–L*). Another Golgi marker, wave18R/mCherry-Got1p (23), showed highly similar distance distributions (median 463 nm with EPSIN1 and 368 nm with MTV1), corroborating the robustness of the center–center distance method (*SI Appendix*, Fig. S4). Taken together, our results strongly suggest that both EPSIN1 and MTV1 are localized at the TGN but that there might be also subtle differences between their respective localizations.

EPSIN1 and MTV1 Play Synergistic Roles in Vacuolar Transport. MTV1 has been demonstrated to be required for vacuolar transport (18), and some data point to an involvement of EPSIN1 in vacuolar transport as well (16). To address whether there are synergistic effects, we quantitatively analyzed transgenic and endogenous vacuolar cargo in *eps1* and *mtv1* single and double mutants. The vacuolar

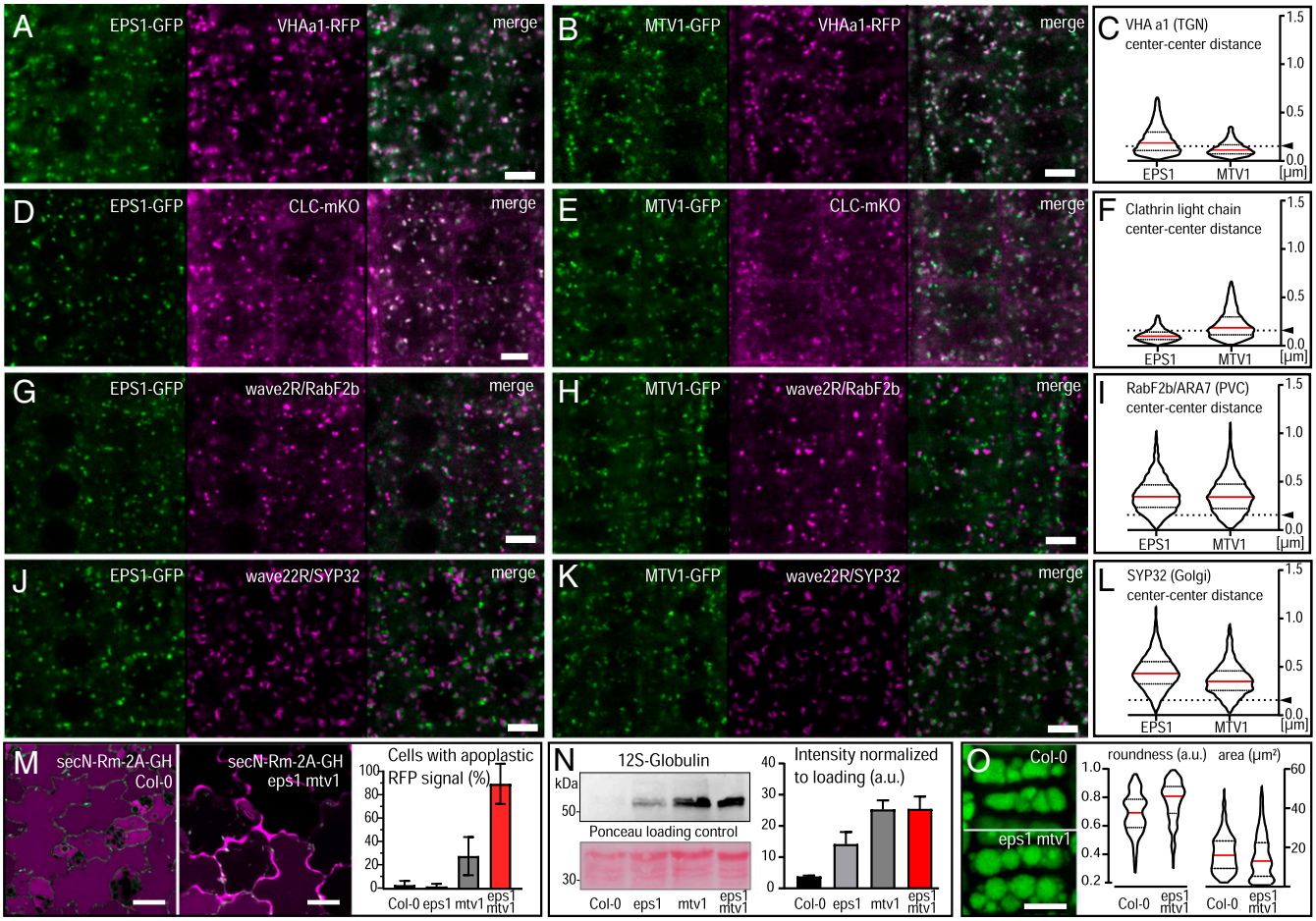

Fig. 2. EPSIN1 and MTV1 reside at the TGN and control vacuolar transport. (*A–L*) Colocalization of EPSIN1-GFP and MTV1-GFP with various subcellular marker lines. Enhanced-resolution (Airyscan) micrographs, object-based quantification of center–center distances, and violin plots of distributions with medians in red and quartiles as dashed lines. The horizontal dashed lines indicate the theoretical resolution limit of ~150 nm. (*A–C*) Colocalization with the TGN marker VHA-a1-RFP. (*D–F*) Colocalization with the clathrin marker CLC2-mKO. (*G–I*) No apparent colocalization with the PVC marker wave2R/mCherry-RabF2b/ARA7. (*J–L*) No clear colocalization with the Golgi marker wave22R/mCherry-SYP32. (*M*) Apoplastic mislocalization of the vacuolar marker SecN-Rm-2A-GH: micrographs of 7 dag cotyledons and plot showing the percentage of cells with apoplastic signal; bars indicate SD, with 227 to 299 cells total per genotype. (*N*) Accumulation of unprocessed 12S storage protein precursors: representative immunoblot and loading control; the graph shows signal quantification as the mean of two independent experiments, and bars indicate SD. (*O*) Altered morphology of storage vacuoles in seed cotyledon parenchyma cells; PSVs are more rounded and smaller in the *eps1 mtv1* double mutant. See *SI Appendix, Materials and Methods* for quantification and statistical details. [Scale bars, 5 µm (*A–K*) and 10 µm (*M* and *O*).]

marker secN-Rm-2A-GH (24) is an RFP fusion protein that normally accumulates in vacuoles. When vacuolar transport is impaired, RFP is secreted via bulk flow into the apoplast. While loss of EPSIN1 had no discernible effects on secN-Rm-2A-GH distribution, loss of MTV1 led to an increased percentage (roughly 25%) of cells with an apoplastic signal. Interestingly, the percentage drastically increased to about 90% in the double mutant (Fig. 2*M*). This suggests that there is a strong synergistic effect of *EPSIN1* and *MTV1* on the vacuolar transport of this marker.

The situation for endogenous vacuolar cargo proved similar: 12S globulin is normally processed en route to the vacuole from a precursor of ∼55 kDa, and accumulation of the precursor form is a well-established indicator of vacuolar transport defects (25). Seed extracts revealed clearly elevated levels of 12S globulin precursor proteins in both the single as well as double mutants, again with *eps1* mutation having the smallest effects (Fig. 2*N*). Interestingly, in *mtv1* single mutants, 12S precursors accumulate almost to the level of the double mutant, while the *epsin1* mutation has only a relatively minor impact. This is most likely related to differences in spatiotemporal expression: *MTV1* expression peaks toward late stages of seed development, when also expression of storage proteins is highest. In contrast, *EPSIN1* expression steadily decreases and is lowest in the late stages (*SI Appendix*, Fig. S5 *A* and *B*). Therefore, loss of *mtv1* would have a much larger impact on storage protein sorting, which occurs at the late stages. Additionally, we observed smaller and more rounded protein storage vacuoles (PSVs) in seeds of the double mutants (Fig. 2*O*). This phenotype is linked to defective vacuolar transport (18) and can be observed also in the single mutants, again with *mtv1* having a stronger effect than *epsin1* (*SI Appendix*, Fig. S5 *C–E*). We conclude that both EPSIN1 as well as MTV1 contribute individually but also synergistically to the transport of at least a subset of vacuolar cargo. Whether this indicates functional redundancy within the same molecular pathway or two independent pathways acting in parallel remains to be determined.

EPSIN1 and MTV1 Contribute to Secretory Transport of a Subset of Cargo. Apart from vacuolar trafficking, secretory transport is another major transport route branching off at the TGN. We tested if *EPSIN1* or *MTV1* plays a role in secretory transport by probing chimeric and endogenous cargo. Sec-RFP is secreted to the apoplast and is an established marker for secretory transport (26). We did not observe obvious differences in apoplastic Sec-RFP signal between the wild type and the double mutant (Fig. 3*A*), indicating no major contribution of EPSIN1 or MTV1 to this transport pathway. Another, endogenous cargo of the secretory pathway is the pectinic mucilage of the seed coat, and a reduced mucilage layer upon seed hydration has been used as a proxy for secretory defects (27). In contrast to unaltered Sec-RFP secretion, we found a clear reduction of mucilage layer thickness, which was mildest in the *eps1* single mutant and strongest in the *eps1 mtv1* double mutant (Fig. 3*B*). This indicates that both EPSIN1 and MTV1 contribute to the transport of a subset of secretory cargo.

EPSIN1 and MTV1 Pathways Are Independent of the TGN Protein ECHIDNA. Of note, the observed mucilage defects were not as strong as in the *echidna* (*ech*) mutant, which we included for reference. ECHIDNA has primarily been implicated in the formation of secretory vesicles at the TGN, but its loss of function also leads to overall alterations of TGN structure, such as a reduction of TGN bulbs and a larger distance between Golgi stacks and the TGN (28). Recent evidence also suggests an involvement of ECHIDNA in vacuolar transport and morphogenesis (29) and loss of ECHIDNA has been shown to cause mislocalization of TGN marker proteins such as VHAa1-RFP into ring-like structures of likely vacuolar/provacuolar nature (28). We have observed a similar phenomenon in the *eps1 mtv1* double mutant for VHAa1-RFP and cyan fluorescent protein-SYP61 (*SI Appendix*, Fig. S6). For these reasons, we wanted to assess whether the observed defects in the *eps1 mtv1* double mutant arise from an interference with an ECHIDNA-dependent pathway. First, we observed the structure of the TGN in the *eps1 mtv1* double mutants by transmission electron microscopy (TEM). We did not detect any notable defects, as the extent of the TGN appeared unaltered, as well as the distance to the Golgi stacks (Fig. 3*C*). We next tested whether loss of EPSIN1 and MTV1 function affected ECH abundance or localization by immunofluorescence employing a specific anti-ECH antibody (28). We did not detect differences in ECH fluorescence intensity and still observed a punctate ECH-positive pattern indistinguishable from wild type in the *eps1 mtv1* double mutant (Fig. 3*D*). Furthermore, we tested whether the structural and functional changes inflicted on the TGN by loss of *ech* had implications for EPSIN1 or MTV1 abundance or localization. We produced affinity-purified antibodies against EPSIN1 and MTV1 (*SI Appendix*, Fig. S7) (18) and compared signals in wild type versus the *ech* mutant. We could not detect any differences regarding signal strength or localization (Fig. 3 *E* and *F*), indicating that *ECH* is not required for EPSIN1 and MTV1 placement. In summary, our data show that EPSIN1 and MTV1 contribute to vacuolar transport and also to the transport of a subset of secretory cargo but EPSIN1 and MTV1 localization is independent of ECH.

EPSIN1 and MTV1 Do Not Contribute to Endocytosis or Endocytic Recycling. In line with their assumed roles in CCV formation, both EPSIN1 and MTV1 have previously been reported to associate with the clathrin heavy chain (16, 18). CCVs are involved in transport processes from and to the PM, and we therefore tested whether EPSIN1 and MTV1 play a role in these processes. We first tested endocytic uptake by quantitatively assessing internalization of the endocytic tracer dye FM4-64. We observed FM4-64 fluorescence after 5 min of incubation and quantified the intensity and number of endosomal structures. The average number of detected FM4-64–positive structures per cell was essentially the same for wild type (Col-0: 20.68 particles per cell, SD 3.8; *eps1 mtv1*: 19.28 particles per cell, SD 4.6; $418 < n < 583$ cells measured). Also, intensity distributions were virtually identical between wild type and the *eps1 mtv1* double mutant (Fig. 3*G*), indicating no difference in endocytic FM4-64 uptake.

To further corroborate these findings, we made use of the transmembrane protein PIN2-GFP. It is constantly endocytosed and recycled back to the PM and has been used as a marker for endocytosis and recycling (30, 31). We first measured PIN2-GFP signal intensity at the PM in wild type and the *eps1 mtv1* double mutant but did not observe a difference (Fig. 3*H*), indicating that PIN2 endocytosis and/or recycling are not likely affected in *eps1 mtv1*.

To distinguish between endocytic and recycling events, we treated PIN2-GFP plants with the fungal toxin brefeldin A (BFA), which inhibits the recycling of internalized material and in *Arabidopsis* root cells leads to accumulation of endocytosed material in endosomal aggregations [so-called BFA compartments (32)]. This has previously been established as a sensitive indicator for defects in PIN2 endocytic trafficking (31, 33). As a quantitative readout, we classified epidermal cells by the number of contained BFA compartments and observed no obvious differences in frequency distribution between Col-0 and *eps1 mtv1* (Fig. 3*I*). Quantifying the intensity of BFA compartments relative to PM localized signal also revealed no obvious differences (*SI Appendix*, Fig. S8), further corroborating the FM4-64 results. An influence on the recycling pathway was tested by measuring PIN2-GFP intensity distribution at the PM after washing out

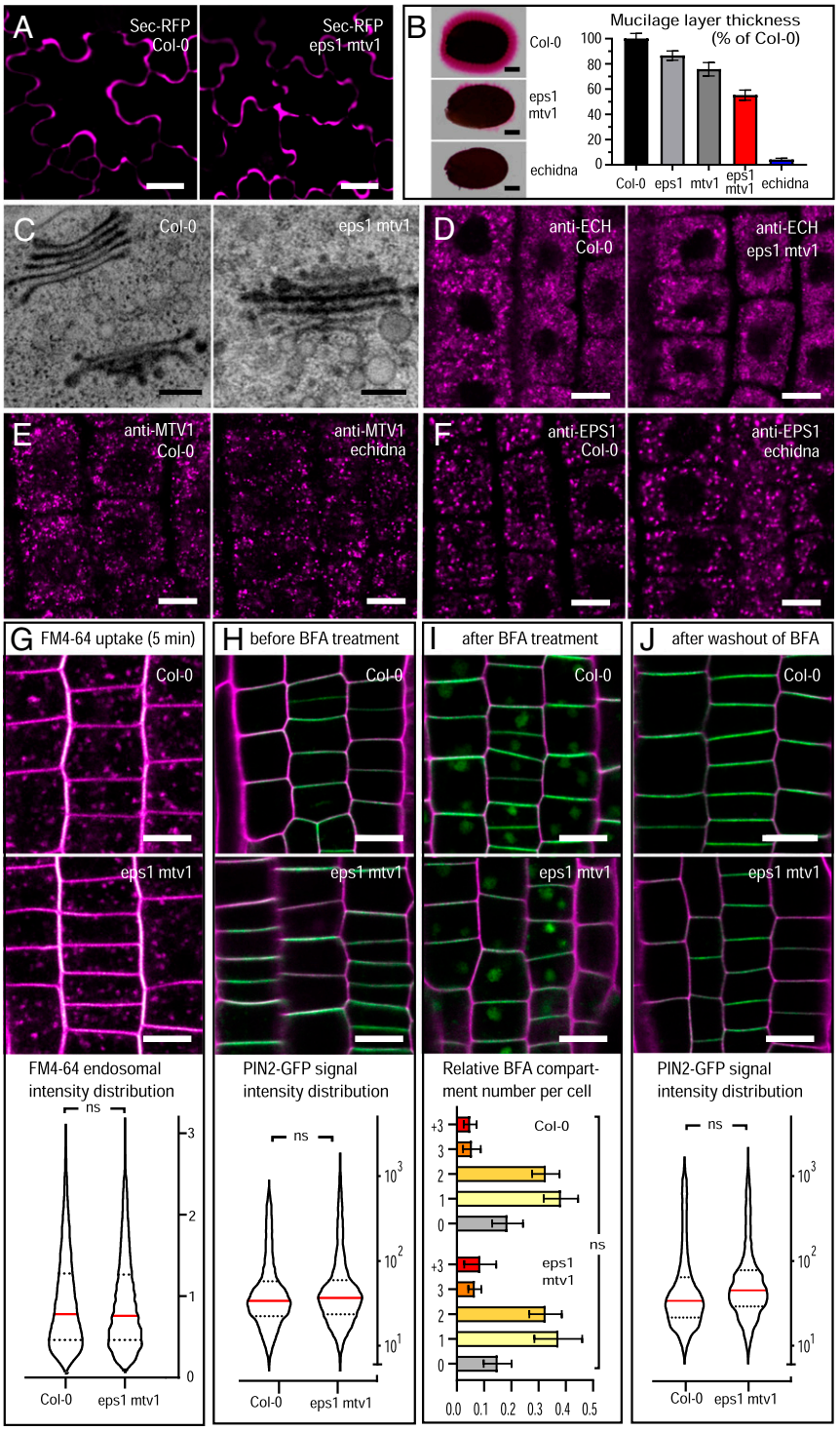

Fig. 3. Differential involvement of *EPSIN1* and *MTV1* in nonvacuolar TGN-dependent trafficking pathways. (*A* and *B*) Defects in trafficking of a subset of secretory cargo. (*A*) The secretory marker Sec-RFP is correctly transported in the *eps1 mtv1* double mutant: micrographs of 7 dag cotyledons. (*B*) Secreted pectinic seed mucilage is stained by ruthenium red after imbibing. Mucilage layer thickness is reduced in *eps1, mtv1*, and the double mutant; secretory mutant *echidna* is shown for comparison. The graph shows mucilage thickness relative to Col-0, and bars indicate 95% CI. (*C*) Golgi and TGN morphology are seemingly unaffected in the *eps1 mtv1* double mutant. Transmission electron micrographs after high-pressure freezing. (*D*) ECHIDNA immunolocalization in *eps1 mtv1* double mutants reveals no obvious localization defects. (*E* and *F*) Loss of ECHIDNA does not affect EPSIN1 or MTV1 localization as revealed by immunolocalization experiments. (*G–J*) EPSIN1 and MTV1 play no apparent role in endocytosis or recycling. (*G*) Endocytic FM4-64 uptake after 5 min: highly similar distribution of endosomal intensity values. (*H*) PIN2-GFP signal before treatment with BFA: highly similar intensity distribution. (*I*) PIN2-GFP signal after 1 h of cotreatment with 50 μM BFA and 50 μM CHX. The graph shows the relative number of cells classified by number of BFA compartments; error bars indicate SD. See also *SI Appendix*, Fig. S8. (*J*) PIN2-GFP signal after a 2-h washout in the presence of 50 μM CHX after previous BFA treatment: highly similar intensity distribution. Refer to *SI Appendix, Materials and Methods* for details. ns, not significant. [Scale bars, 10 μm (*A* and *D–J*), 100 μm (*B*), and 200 nm (*C*).]

BFA in the presence of the translation elongation inhibitor cycloheximide (CHX) to block de novo synthesis. We found a nearly complete restoration of PIN2-GFP at the PM with no significant differences in signal intensity distribution between the double mutant and wild type (Fig. 3*J*). Taken together, our results suggest that MTV1 and EPSIN1 do not significantly contribute to endocytic or recycling transport routes.

EPSIN1 and MTV1 Are Spatially Separated. From the data, one could speculate that EPSIN1 and MTV1 perform largely overlapping functions at the TGN by synergistically acting on the same molecular pathway. Such a hypothesis, however, would raise the question of whether these two phylogenetically rather divergent proteins (Fig. 1*A*) indeed impinge on the same molecular machinery, or whether their different lineage might be reflected at

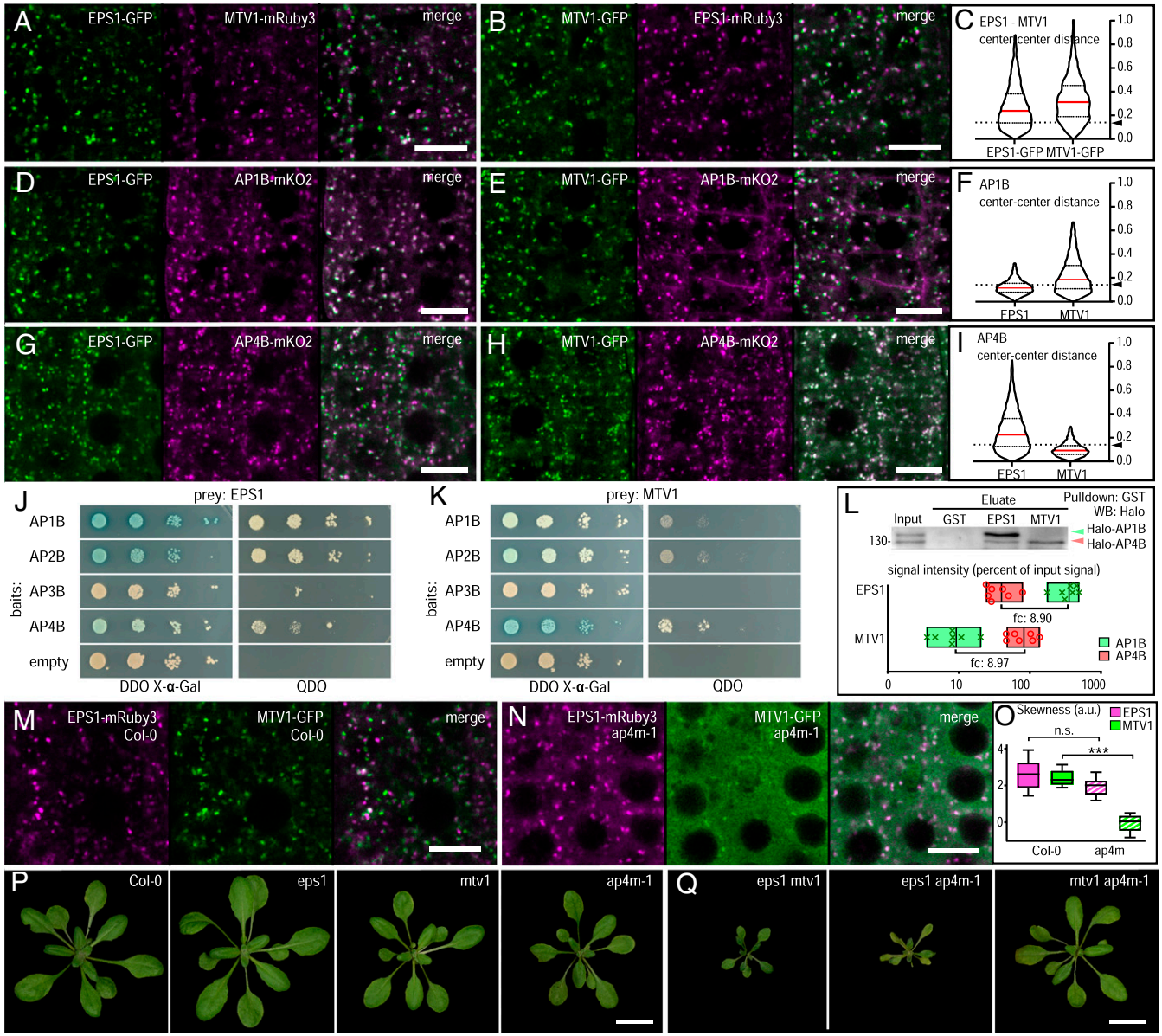

Fig. 4. EPSIN1/AP-1 and MTV1/AP-4 define two spatially and molecularly distinct TGN subdomains. (*A–C*) Colocalization of EPSIN1-GFP with MTV1-mRuby3 (*A*) or EPSIN1-mRuby3 with MTV1-GFP (*B*) reveals a relatively large distance between EPSIN1- and MTV1-positive domains. (*D–F*) EPSIN1 preferentially colocalizes with AP-1B. (*G–I*) MTV1 preferentially colocalizes with AP-4B. (*J* and *K*) Yeast two-hybrid assay showing the strongest interactions between EPSIN1 and AP-1B (*J*) and MTV1 and AP-4B (*K*). (*L*) Competitive in vitro interaction. In the presence of equimolar amounts of AP-1B and AP-4B, EPSIN1 preferentially pulls down AP-1B and MTV1 pulls down AP-4B. Representative immunoblot and scatterplot of signal quantification (relative to input intensity) from three independent pull-down assays with two or three technical replicates each. Bars indicate range and mean. WB, Western blotting. See also *SI Appendix*, Fig. S10. (*M–O*) MTV1, but not EPSIN1, localization requires the AP-4 complex. (*M*) EPSIN1-mRuby3 and MTV1-GFP punctae in the wild-type background. (*N*) Loss of MTV1-GFP, but not EPSIN1-mRuby3, punctae in the *ap4m* mutant. (*O*) Quantification of the presence of defined punctate signal by analyzing the skewness of the signal intensity of 10 independent point populations of 2,000 measurements each; higher skewness indicates more punctate signal, and lower skewness a more diffuse signal. ***$P < 0.001$. Please refer to *SI Appendix, Materials and Methods* for a detailed explanation. (*P* and *Q*) Genetic interaction between MTV1 and AP-4: rosette phenotype at 25 dag. (*P*) Phenotypes of *eps1*, *mtv1*, and *ap4m* single mutants. Note the smaller rosettes of the latter two. (*Q*) The dwarf phenotype of the *eps1 mtv1* double mutant is phenocopied by *eps1 ap4m* while *mtv1 ap4m* shows no genetic interaction. Refer to *SI Appendix, Materials and Methods* for details. Horizontal dotted lines in *C*, *F*, and *I* indicate the theoretical resolution limit at 150 nm. Number of object pairs scored in *A–I*: 5,038 < *n* < 8,798. [Scale bars, 10 μm (*C–N*) and 2 cm (*P* and *Q*).]

the levels of localization, molecular interaction, and/or function. The observation that EPSIN1 and MTV1 displayed subtle differences in their localization distances relative to the TGN markers (Fig. 2) prompted us to investigate EPSIN1 and MTV1 colocalization. To this end, we generated additional, functional mRuby3-tagged versions of both proteins expressed under control of their endogenous promoters and analyzed co-occurrence of each with the respective GFP-tagged counterparts. Center–center distance analysis yielded median values higher than those observed for co-occurrence with TGN markers (median 230 and 292 nm, compared with values below 200 nm for all TGN markers tested) (Fig. 4 *A–C*). These values were above the optical resolution limit and separation was already clearly visible in the micrographs, indicating that MTV1 and EPSIN1 mark distinct entities. Given that both are bona fide TGN-associated proteins, this strongly suggests their presence at two distinct TGN subdomains.

EPSIN1/AP-1 and MTV1/AP-4 Define Two Separate TGN Subdomains. We reasoned that these hypothetical EPSIN1- and MTV1-positive subdomains might be molecularly further distinguishable by co-occurrence of preferred interaction partners. EPSIN1 has previously been shown to interact with the AP-1 complex (16). On the other hand, tepsin, an only distantly related MTV1 ortholog present in animal systems, binds the AP-4 complex via the appendage domain of the AP-4 beta subunit (34). We therefore generated mKO2-tagged versions of the beta subunits of AP complexes 1 and 4 (AP-1B and AP-4B) under their endogenous promoters and tested their co-occurrence with EPSIN1-GFP or MTV1-GFP, respectively. Strikingly, we observed clearly distinguishable distance distribution patterns: EPSIN1 preferentially colocalized with AP-1B (median distance 117 nm) and displayed a nearly twice larger distance to AP-4B (median 225 nm), whereas MTV1 colocalized strongly with AP-4B (median distance 92 nm) but was located clearly farther away from AP-1B (median distance 191 nm) (Fig. 4 *D–I*). Between 6,981 and 8,797 object pairs from at least 10 roots were measured (see *SI Appendix*, Table S2 for detailed numbers).

We next addressed whether the closer subcellular association of the EPSIN1/AP-1 and MTV1/AP-4 pairs might be reflected at the level of their molecular interactions. ENTH proteins typically interact with AP complexes through the appendage domains of the beta subunits (34). We therefore probed protein–protein interactions between the beta subunits of the AP-1, AP-2, AP-3, and AP-4 complexes (expressed as baits) and EPSIN1 and MTV1 (expressed as preys) in yeast two-hybrid (Y2H) assays. In accordance with the subcellular localization results, the strongest interactions were observed for the EPSIN1/AP-1B and MTV1/AP-4B pairs (Fig. 4 *J* and *K*). It should be noted that these interactions were not exclusive and weaker interactions were observed with other AP beta subunits, especially between EPSIN1 and AP-2B. This is, however, not surprising because β-adaptin isoforms of AP-1 and AP-2 are shared proteins in both complexes (35, 36). In order to test these findings also in planta, we extended our co-occurrence analyses to mKO2-tagged versions of AP-2B and AP-3B (*SI Appendix*, Fig. S9). Here, EPSIN1 colocalized nearly perfectly with the punctate signal population of AP-2B (median 64 nm), which pertains to the AP-2B subunit incorporated into the AP-1 complex, while MTV1 was clearly much farther away (median 265 nm) (*SI Appendix*, Fig. S9 *A–C*). For AP-3B, neither EPSIN1 (median 352 nm) nor MTV1 (median 260 nm) was noticeably close (*SI Appendix*, Fig. S9 *D–F*). These data are fully in line with the Y2H results and further support the notion of EPSIN1 preferentially binding the AP-1 complex and MTV1 preferentially binding AP-4.

In order to further probe the binding preferences of EPSIN1 and MTV1, we performed a competitive in vitro pull-down assay, using an equimolar mix of cell-free expressed HaloTag-AP-1B and HaloTag-AP-4B as binding partners for glutathione-agarose–bound glutathione S-transferase (GST)-EPSIN1 and GST-MTV1, with GST as negative control. We performed and quantified three independent pull-down assays with two or three technical replicates each. We found that GST alone did not pull down any detectable HaloTag protein, while GST-EPSIN1 preferentially pulled down HaloTag-AP-1 (on average 8.9-fold more signal than for HaloTag-AP-4B), and GST-MTV1 preferentially pulled down HaloTag-AP-4B (on average 9-fold more signal than HaloTag-AP-1B) (Fig. 4*L* and *SI Appendix*, Fig. S10).

Taken together, these three complementary approaches suggest a preferential subcellular association and molecular interaction of EPSIN1 with AP-1 and of MTV1 with AP-4.

AP-4 Recruits MTV1 and Both Act in the Same Molecular Pathway. In light of the MTV1–AP-4 colocalization and protein–protein interaction, we aimed to address the relevance of this interaction in planta. To this end, we first tested localization of EPSIN1 and MTV1 to endosomal structures in an *ap4m* mutant (36) lacking the small μ-subunit of AP-4, which disrupts the entire complex. Intriguingly, loss of AP-4 complex function led to an almost complete abolishment of the MTV1-GFP punctate pattern, which remained mostly cytosolic in the *ap4m* mutant (Fig. 4 *M–O*), whereas the punctate EPSIN1-mRuby signal remained largely unaffected (Fig. 4 *M–O*). This suggests that a functional AP-4 complex is specifically required for either MTV1 recruitment or its stabilization at the TGN. Although EPSIN1-mRuby signal was essentially unaltered in the *ap4m* mutant, we further wanted to verify that the observed defects were not due to a general alteration of the TGN in the *ap4m* mutant. For this, we quantified the size and shape of the TGN by using immunolocalization of ECHIDNA as a marker for the overall TGN, followed by DiAna object-based detection and quantification. Neither visual inspection nor image quantification results revealed any marked difference in size or overall shape (*SI Appendix*, Fig. S11). Therefore, a general disruptive effect of *ap4m* on the TGN seems unlikely.

The different effects of loss of AP-4 on EPSIN1 and MTV1 prompted us to examine genetic interactions, especially since loss of the *Arabidopsis* AP-4 complex causes slightly reduced leaf rosette size (36), similar to what we observed in *mtv1* mutants (Figs. 1*C* and 4*P* and *SI Appendix*, Fig. S2). Given the strong dependence of MTV1 localization on AP-4 function, we predicted that if *MTV1* and *AP-4* act in the same pathway, loss of *AP-4* activity should phenocopy loss of *MTV1*, and *mtv1* mutations should not enhance the *ap4m* mutant phenotype. To test this and to compare it with a putative interaction with *EPSIN1*, we generated *mtv1 ap4m* and *eps1 ap4m* double mutants. As expected, *mtv1* and *ap4m* single mutants displayed reduced rosette size phenotypes that were indistinguishable from each other (Fig. 4*P*) and also from the *mtv1 ap4m* double mutant (Fig. 4*Q*), further supporting that *AP-4* and *MTV1* act in the same pathway. Strikingly, and in support of this view, both the *mtv1* and the *ap4m* mutations strongly enhanced the *eps1* phenotype. Both the *mtv1 eps1* and *ap4m eps1* double mutants cause an indistinguishable dwarf phenotype (Fig. 4*Q*). Thus, our findings strongly support that AP-4 and MTV1 act in the same molecular pathway, which is molecularly distinct from EPSIN1. However, the functions of these two pathways largely overlap, resulting in a strongly synergistic genetic interaction upon mutation of members in both pathways.

Discussion

EPSIN1 and MTV1 Are the Major ENTH Proteins at the TGN and Promote Vacuolar and Secretory Transport. We identified EPSIN1 and MTV1 as the two major ENTH proteins present at the TGN by analyzing functional redundancy among all large *Arabidopsis* ENTH proteins. Their simultaneous loss of function leads to

defects in vacuolar and secretory transport, ultimately resulting in drastic overall growth defects. This indicates that EPSIN1 and MTV1 form a functionally redundant, or at least widely overlapping, pair, whose function cannot be adequately replaced by any other molecular component.

Previous results on EPSIN1 were limited to a partial loss-of-function mutant (SALK_049204). The *eps1* full loss-of-function allele used in this study (SAIL_394G02) also shows noticeable, albeit relatively weak, vacuolar transport defects. In line with this, the EPSIN1 ortholog from mammals, Epsin1R, also has a clear but limited contribution to vacuolar/lysosomal transport (37, 38). MTV1, on the other hand, has a much stronger impact on all tested vacuolar markers. Interestingly, however, the combination of *eps1* and *mtv1* mutations leads to defects in vacuolar transport that go much beyond an additive defect, as exemplified by the vacuolar marker sec-N-Rm-2A (Fig. 2*M*). This could indicate that 1) EPSIN1 and MTV1 mutually act in the same molecular pathway and are direct functional replacements of one another or 2) there are two independent pathways with overlapping cargo. Our association data with AP-1 and AP-4 (see below) strongly support the latter explanation.

We were surprised about the secretory defects observed in the *eps1* and *mtv1* mutants, because previous reports did not hint at an involvement of either protein in secretory activity (16, 18). However, a very recent study supports our findings, in that EPSIN1 does contribute to anterograde PM transport of a subset of membrane proteins (17). Generally, the role of the plant TGN in secretory activity is well-established and a number of molecular components, such as SYP42/43, SYP61, ECHIDNA, and YIP4A/B, are known players in secretory transport from the TGN (reviewed in refs. 39 and 40). In particular, the transport of cell-wall components has gained attention, and seed coat mucilage has become an established model to study biosynthesis and secretory pathways of extracellular polysaccharides. Mounting evidence suggests several independent pathways for secretion of TGN-derived extracellular cargo (reviewed in ref. 39). Our results support this notion, as the transport of a secretory marker, Sec-RFP, is unaltered in the *eps1 mtv1* double mutant, whereas seed coat mucilage secretion is clearly reduced. However, some caution must be exerted in the interpretation of these results, since the observed organs (cotyledons and seed coat) are very different and activity of different transport pathways may not be directly comparable. We also cannot exclude the possibility that the observed mucilage reduction is due to a down-regulation of biosynthesis. However, the recent finding that the AP-1 complex participates in mucilage transport (41) strongly suggests that ENTH proteins influence secretory events. Since AP-1, EPSIN1, and MTV1 are all clathrin-associated, this implies that mucilage transport can make use of CCVs. However, it is clear that this is not the only pathway for secretion of pectinic polysaccharides, because the *eps1 mtv1* double mutant does not result in full mucilage transport blockage, as observed in the *ech* mutant, for example (27).

EPSIN1 and MTV1 Are Not Directly Related to ECHIDNA-Mediated TGN Stability. The results on secretion and mislocalization of TGN marker proteins prompted us to probe a potential relation to the ECHIDNA protein, which is a major factor required for Golgi–TGN association and secretory function (27, 28, 42). Loss of ECH causes secretory defects associated with changes in TGN morphology and we therefore probed if loss of *eps1* and *mtv1* causes defects in TGN morphology by TEM. However, our results exclude dramatic defects in TGN morphology and, furthermore, in the *eps1 mtv1* double mutant, ECH is still correctly localized, indicating that EPSIN1 and MTV1 are not components merely required for TGN structure. Interestingly, also in *ech* mutants with altered TGN structure and post-Golgi transport defects, EPSIN1 and MTV1 exhibit a punctate localization pattern indistinguishable from the wild-type situation. Hence, proper TGN recruitment or maintenance of the localization of these players does not require *ECH* function.

EPSIN1/AP-1 and MTV1/AP-4 Define Two TGN Subdomains. Mounting evidence suggests that the diverse transport routes branching at the TGN of plants pertain to subdomains or subpopulations of distinct molecular makeup (e.g., refs. 3, 4, 6, and 7). We have now identified two spatially distinct subdomains of the plant TGN by microscopic interaction and genetic analyses. One domain preferentially contains AP-1 and EPSIN1 and the other one contains AP-4 and MTV1. MTV1 is furthermore dependent on recruitment by the AP-4 complex and loss of either the AP-4 complex or MTV1 has a similar functional outcome. This suggests that AP-4/MTV1 are indispensable players in a transport pathway that is molecularly independent of AP-1/EPSIN1.

Nevertheless, our data also indicate that the two pathways overlap functionally and likely contribute to vacuolar and secretory transport of a similar subset of cargo. This is supported by previous findings that the AP-4 complex and MTV1 are clearly linked to vacuolar transport and secretion of a subset of cargo (18, 37, 43, 44). The plant AP-1 complex has broad functionality in post-Golgi secretory and vacuolar traffic during interphase as well as cytokinesis, and notably also mucilage secretion (42, 45–47). Loss of AP-1 is gametophytic lethal, underscoring its importance in a wide range of transport processes. EPSIN1, on the other hand, appears to play a more specific role, as its loss does not cause severe phenotypes. Consequently, AP-1 may not be strictly dependent on EPSIN1 but instead may function without accessory proteins, or with other members of the related ANTH domain protein family (15). Our Y2H and in vitro interaction data suggest that at least in these heterologous systems, EPSIN1 can also interact with AP-4, although to a small extent, and the same holds true for MTV1 and AP-1. We therefore do not rule out that there is some level of direct functional replacement between EPSIN1 and MTV1, possibly at the level of AP complex choice.

AP-4 Interaction with MTV1/Tepsin Is Evolutionarily Conserved. MTV1 clearly differs from animal tepsin in that it was found enriched in CCVs and binds the clathrin heavy chain via its unstructured C-terminal half (18). Intriguingly, for tepsin there is no evidence of a clathrin association, as the AP-4 complex in animal systems is believed to be a nonclathrin coat (48, 49). Nevertheless, the fact that MTV1 and tepsin require AP-4 for endosomal recruitment appears to be a feature conserved between animals and plants (this study and ref. 31), and the amino acid motifs for tepsin–AP-4B interactions (50, 51) are also present in MTV1. This suggests that the interaction between MTV1/tepsin and the AP-4 complex remained evolutionarily conserved, but the function and clathrin dependency of the AP-4 complex may have evolved independently. In animals, the exact roles of AP-4 and tepsin for trafficking events remain to be determined. AP-4 has been implicated in anterograde TGN endosomal sorting of basolateral PM cargo as well as amyloid precursors and its loss causes neurological defects in humans (reviewed in ref. 52). A direct role for AP-4 in lysosomal transport has not been demonstrated. Interestingly, a recent study links animal AP-4 to autophagic events because the core component ATG9A is not properly exported from the TGN to the cytosol in AP-4–deficient cells (53). Loss of tepsin, on the other hand, did not affect ATG9A sorting, indicating that not all functions of animal AP-4 require this accessory protein. Whether plant AP-4 and/or MTV1 also participate in autophagic events can now be addressed in future studies.

Conclusion

Our results demonstrate that EPSIN1 and MTV1 are the two major ENTH-type accessory proteins at the TGN involved in vacuolar and secretory transport. Although the phenotypes observed upon mutation of both pathways are largely overlapping and often a genetic enhancement is observed, the two pathways in which EPSIN1 and MTV1 play a role appear to be distinct based on both subcellular localization and molecular interaction data. They can be molecularly defined by association with two different AP complexes and occur at spatially and molecularly separated regions of the TGN. Our work thus provides an important molecular stepping stone for future studies defining additional TGN subdomains and for in-detail probing of the relationships between the different APs and their accessory proteins in specifying the still largely enigmatic plant TGN.

Materials and Methods

Functionality of pEPSIN1:EPSIN1-GFP and pMTV1:MTV1-GFP constructs was verified in several complementation assays (*SI Appendix*, Fig. S12). All lines and materials are described in *SI Appendix, Materials and Methods*. *Arabidopsis* plants were grown under a 16/8-h, 23/18 °C, light/dark cycle on soil or vertical agar plates with 1% sucrose Murashige and Skoog medium at pH 5.8. All confocal microscopy was performed on a Zeiss LSM 880 Airyscan Fast System. Protein–protein interactions were done using the Matchmaker Gold Y2H assay or via pull-down experiments using HaloTag-coupled bait and GST-coupled prey. Please refer to *SI Appendix, Materials and Methods* for a detailed description of all experimental procedures and the statistical analyses employed.

Data Availability. Original imaging files are available upon request.

ACKNOWLEDGMENTS. This research was funded by Deutsche Forschungsgemeinschaft Grants SA2427/2-1 (to M.S.) and INST 336/114-1 FUGG for large equipment to Markus Grebe and coapplicants. H.E.M. acknowledges an Australian Research Council Discovery Early Career Researcher Award (DE170100054) and support from the Canada Research Chairs Program. Electron microscopy was conducted using equipment at the University of Melbourne Advanced Microscopy Facility. We are very grateful to M. Grebe for support and discussion throughout the project. We thank K. A. for expert technical support and J. Kleine-Vehn and M. Grebe for critical reading of the manuscript. *ech* mutant seeds and purified ECHIDNA antibody were kind gifts from R. Bhalerao, and 2S and 12S globulin antibodies were generously provided by T. Shimada. We acknowledge the Nottingham *Arabidopsis* Stock Centre and Addgene for distribution of seeds and plasmids.

1. L. A. Staehelin, T. H. Giddings Jr., J. Z. Kiss, F. D. Sack, Macromolecular differentiation of Golgi stacks in root tips of *Arabidopsis* and *Nicotiana* seedlings as visualized in high pressure frozen and freeze-substituted samples. *Protoplasma* **157**, 75–91 (1990).
2. T. Uemura, Physiological roles of plant post-Golgi transport pathways in membrane trafficking. *Plant Cell Physiol.* **57**, 2013–2019 (2016).
3. G. Drakakaki *et al*., Isolation and proteomic analysis of the SYP61 compartment reveal its role in exocytic trafficking in *Arabidopsis*. *Cell Res.* **22**, 413–424 (2012).
4. V. Wattelet-Boyer *et al*., Enrichment of hydroxylated C24- and C26-acyl-chain sphingolipids mediates PIN2 apical sorting at *trans*-Golgi network subdomains. *Nat. Commun.* **7**, 12788 (2016).
5. R. Ravikumar *et al*., Independent yet overlapping pathways ensure the robustness and responsiveness of *trans*-Golgi network functions in *Arabidopsis*. *Development* **145**, dev169201 (2018).
6. L. Renna *et al*., TGNap1 is required for microtubule-dependent homeostasis of a subpopulation of the plant *trans*-Golgi network. *Nat. Commun.* **9**, 5313 (2018).
7. T. Uemura *et al*., A Golgi-released subpopulation of the *trans*-Golgi network mediates protein secretion in *Arabidopsis*. *Plant Physiol.* **179**, 519–532 (2019).
8. J. Hirst *et al*., The fifth adaptor protein complex. *PLoS Biol.* **9**, e1001170 (2011).
9. M. K. Singh, G. Jürgens, Specificity of plant membrane trafficking—ARFs, regulators and coat proteins. *Semin. Cell Dev. Biol.* **80**, 85–93 (2018).
10. D. J. Owen *et al*., A structural explanation for the binding of multiple ligands by the α-adaptin appendage domain. *Cell* **97**, 805–815 (1999).
11. M. G. Ford *et al*., Curvature of clathrin-coated pits driven by epsin. *Nature* **419**, 361–366 (2002).
12. M. Messa *et al*., Epsin deficiency impairs endocytosis by stalling the actin-dependent invagination of endocytic clathrin-coated pits. *eLife* **3**, e03311 (2014).
13. M. A. Zhukovsky, A. Filograna, A. Luini, D. Corda, C. Valente, Protein amphipathic helix insertion: A mechanism to induce membrane fission. *Front. Cell Dev. Biol.* **7**, 291 (2019).
14. A. Sen, K. Madhivanan, D. Mukherjee, R. C. Aguilar, The epsin protein family: Coordinators of endocytosis and signaling. *Biomol. Concepts* **3**, 117–126 (2012).
15. J. Zouhar, M. Sauer, Helping hands for budding prospects: ENTH/ANTH/VHS accessory proteins in endocytosis, vacuolar transport, and secretion. *Plant Cell* **26**, 4232–4244 (2014).
16. J. Song, M. H. Lee, G.-J. Lee, C. M. Yoo, I. Hwang, *Arabidopsis* EPSIN1 plays an important role in vacuolar trafficking of soluble cargo proteins in plant cells via interactions with clathrin, AP-1, VTI11, and VSR1. *Plant Cell* **18**, 2258–2274 (2006).
17. C. A. Collins *et al*., EPSIN1 modulates the plasma membrane abundance of FLAGELLIN SENSING2 for effective immune responses. *Plant Physiol.* **182**, 1762–1775 (2020).
18. M. Sauer *et al*., MTV1 and MTV4 encode plant-specific ENTH and ARF GAP proteins that mediate clathrin-dependent trafficking of vacuolar cargo from the *trans*-Golgi network. *Plant Cell* **25**, 2217–2235 (2013).
19. G.-J. Lee *et al*., EpsinR2 interacts with clathrin, adaptor protein-3, AtVTI12, and phosphatidylinositol-3-phosphate. Implications for EpsinR2 function in protein trafficking in plant cells. *Plant Physiol.* **143**, 1561–1575 (2007).
20. J.-F. Gilles, M. Dos Santos, T. Boudier, S. Bolte, N. Heck, DiAna, an ImageJ tool for object-based 3D co-localization and distance analysis. *Methods* **115**, 55–64 (2017).
21. J. Dettmer, A. Hong-Hermesdorf, Y.-D. Stierhof, K. Schumacher, Vacuolar H^+-ATPase activity is required for endocytic and secretory trafficking in *Arabidopsis*. *Plant Cell* **18**, 715–730 (2006).
22. E. Ito *et al*., Dynamic behavior of clathrin in *Arabidopsis thaliana* unveiled by live imaging. *Plant J.* **69**, 204–216 (2012).
23. N. Geldner *et al*., Rapid, combinatorial analysis of membrane compartments in intact plants with a multicolor marker set. *Plant J.* **59**, 169–178 (2009).
24. M. Samalova, M. Fricker, I. Moore, Ratiometric fluorescence-imaging assays of plant membrane traffic using polyproteins. *Traffic* **7**, 1701–1723 (2006).
25. T. Shimada *et al*., Vacuolar sorting receptor for seed storage proteins in *Arabidopsis thaliana*. *Proc. Natl. Acad. Sci. U.S.A.* **100**, 16095–16100 (2003).
26. C. Faso *et al*., A missense mutation in the *Arabidopsis* COPII coat protein Sec24A induces the formation of clusters of the endoplasmic reticulum and Golgi apparatus. *Plant Cell* **21**, 3655–3671 (2009).
27. D. Gendre *et al*., *Trans*-Golgi network localized ECHIDNA/Ypt interacting protein complex is required for the secretion of cell wall polysaccharides in *Arabidopsis*. *Plant Cell* **25**, 2633–2646 (2013).
28. D. Gendre *et al*., Conserved *Arabidopsis* ECHIDNA protein mediates *trans*-Golgi-network trafficking and cell elongation. *Proc. Natl. Acad. Sci. U.S.A.* **108**, 8048–8053 (2011).
29. T. Ichino, K. Maeda, I. Hara-Nishimura, T. Shimada, *Arabidopsis* ECHIDNA protein is involved in seed coloration, protein trafficking to vacuoles, and vacuolar biogenesis. *J. Exp. Bot.* **71**, 3999–4009 (2020).
30. J. Kleine-Vehn *et al*., Differential degradation of PIN2 auxin efflux carrier by retromer-dependent vacuolar targeting. *Proc. Natl. Acad. Sci. U.S.A.* **105**, 17812–17817 (2008).
31. S. Men *et al*., Sterol-dependent endocytosis mediates post-cytokinetic acquisition of PIN2 auxin efflux carrier polarity. *Nat. Cell Biol.* **10**, 237–244 (2008).
32. N. Geldner, J. Friml, Y.-D. Stierhof, G. Jürgens, K. Palme, Auxin transport inhibitors block PIN1 cycling and vesicle trafficking. *Nature* **413**, 425–428 (2001).
33. S. Kitakura *et al*., Clathrin mediates endocytosis and polar distribution of PIN auxin transporters in *Arabidopsis*. *Plant Cell* **23**, 1920–1931 (2011).
34. G. H. H. Borner *et al*., Multivariate proteomic profiling identifies novel accessory proteins of coated vesicles. *J. Cell Biol.* **197**, 141–160 (2012).
35. M. Boehm, J. S. Bonifacino, Adaptins: The final recount. *Mol. Biol. Cell* **12**, 2907–2920 (2001).
36. K. Fuji *et al*., The adaptor complex AP-4 regulates vacuolar protein sorting at the *trans*-Golgi network by interacting with VACUOLAR SORTING RECEPTOR1. *Plant Physiol.* **170**, 211–219 (2016).
37. J. Hirst, A. Motley, K. Harasaki, S. Y. Peak Chew, M. S. Robinson, EpsinR: An ENTH domain-containing protein that interacts with AP-1. *Mol. Biol. Cell* **14**, 625–641 (2003).
38. I. G. Mills *et al*., EpsinR: An AP1/clathrin interacting protein involved in vesicle trafficking. *J. Cell Biol.* **160**, 213–222 (2003).
39. R. Sinclair, M. R. Rosquete, G. Drakakaki, Post-Golgi trafficking and transport of cell wall components. *Front. Plant Sci.* **9**, 1784 (2018).
40. S.-J. Kim, F. Brandizzi, The plant secretory pathway for the trafficking of cell wall polysaccharides and glycoproteins. *Glycobiology* **26**, 940–949 (2016).
41. T. Shimada *et al*., The AP-1 complex is required for proper mucilage formation in *Arabidopsis* seeds. *Plant Cell Physiol.* **59**, 2331–2338 (2018).
42. H. E. McFarlane *et al*., Cell wall polysaccharides are mislocalized to the vacuole in echidna mutants. *Plant Cell Physiol.* **54**, 1867–1880 (2013).

43. D. C. Gershlick *et al*., Golgi-dependent transport of vacuolar sorting receptors is regulated by COPII, AP1, and AP4 protein complexes in tobacco. *Plant Cell* **26**, 1308–1329 (2014).
44. H. Pertl-Obermeyer *et al*., Identification of cargo for adaptor protein (AP) complexes 3 and 4 by sucrose gradient profiling. *Mol. Cell. Proteomics* **15**, 2877–2889 (2016).
45. M. Park *et al*., *Arabidopsis* μ-adaptin subunit AP1M of adaptor protein complex 1 mediates late secretory and vacuolar traffic and is required for growth. *Proc. Natl. Acad. Sci. U.S.A.* **110**, 10318–10323 (2013).
46. O.-K. Teh *et al*., The AP-1 μ adaptin is required for KNOLLE localization at the cell plate to mediate cytokinesis in *Arabidopsis*. *Plant Cell Physiol.* **54**, 838–847 (2013).
47. J.-G. Wang *et al*., HAPLESS13, the *Arabidopsis* μ1 adaptin, is essential for protein sorting at the *trans*-Golgi network/early endosome. *Plant Physiol.* **162**, 1897–1910 (2013).
48. E. C. Dell'Angelica, C. Mullins, J. S. Bonifacino, AP-4, a novel protein complex related to clathrin adaptors. *J. Biol. Chem.* **274**, 7278–7285 (1999).
49. J. Hirst, N. A. Bright, B. Rous, M. S. Robinson, Characterization of a fourth adaptor-related protein complex. *Mol. Biol. Cell* **10**, 2787–2802 (1999).
50. M. N. Frazier *et al*., Molecular basis for the interaction between AP4 β4 and its accessory protein, tepsin. *Traffic* **17**, 400–415 (2016).
51. R. Mattera, C. M. Guardia, S. S. Sidhu, J. S. Bonifacino, Bivalent motif-ear interactions mediate the association of the accessory protein tepsin with the AP-4 adaptor complex. *J. Biol. Chem.* **290**, 30736–30749 (2015).
52. J. Hirst, C. Irving, G. H. H. Borner, Adaptor protein complexes AP-4 and AP-5: New players in endosomal trafficking and progressive spastic paraplegia. *Traffic* **14**, 153–164 (2013).
53. R. Mattera, S. Y. Park, R. De Pace, C. M. Guardia, J. S. Bonifacino, AP-4 mediates export of ATG9A from the *trans*-Golgi network to promote autophagosome formation. *Proc. Natl. Acad. Sci. U.S.A.* **114**, E10697–E10706 (2017).